



Tissue Plasminogen Activator Loaded PCL Nanofibrous Scaffold Promoted Nerve Regeneration After Sciatic Nerve Transection in Male Rats

Ensieh Sajadi^{1,2} · Abbas Aliaghaei² · Reza Mastery Farahni² · Ali Rashidiani-Rashidabadi³ · Amir Raoofi⁴ · Yousef Sadeghi⁵ · Mohammad Bagheri² · Saba Ilkhani² · Mohammad-Amin Abdollahifar^{1,2} 

Received: 28 May 2020 / Revised: 19 August 2020 / Accepted: 20 August 2020
© Springer Science+Business Media, LLC, part of Springer Nature 2020

Abstract

According to the studies, damages to the peripheral nerve as a result of a trauma or acute compression, stretching, or burns accounts for a vast range of discomforts which strongly impressed the patient's life quality. Applying highly potent biomolecules and growth factors in the damaged nerve site would promote the probability of nerve regeneration and functional recovery. Tissue plasminogen activator (tPA) is one of the components that can contribute importantly to degenerating and regenerating the peripheral nerves following the injuries occurred and the absence of this biomolecule hinders the recoveries of the nerves. This technique would guarantee the direct accessibility of tPA for the regenerating axons. Structural, physical, and in vitro cytotoxicity evaluations were done before in vivo experiments. In this study, twenty-four mature male rats have been exploited. The rats have been classified into four groups: controls, axotomy, axotomy + scaffold, and axotomy + tPA-loaded scaffold. Four, 8, and 12 weeks post-surgical, the sciatic functional index (SFI) has been measured. After 12 weeks, the spinal cord, sciatic nerve, and dorsal root ganglion specimens have been removed and stereological procedures, immunohistochemistry, and gene expression have been used to analyze them. Stereological parameters, immunohistochemistry of GFAP, and gene expression of S100, NGF, and BDNF were significantly enhanced in tPA-loaded scaffold group compared with axotomy group. The most similarity was observed between the results of control group and tPA-loaded scaffold group. According to the results, a good regeneration of the functional nerve tissues in a short time was observed as a result of introducing tPA.

Keywords Peripheral nerve · Tissue plasminogen activator · Plasma irradiation · In vivo evaluations · Axonal regeneration

Introduction

Peripheral nerve injuries are common conditions. The cause of these occurrences by trauma and medical interventions may lead to motor, sensory, and autonomic function disabilities or result from medical interventions (Grinsell and Keating 2014). Serious nerve injuries have destructive impacts on the life quality of patients. Common symptoms include deficiencies in the motor and sensory functions that lead to full paralysis of the affected limbs or progression of the intractable neuropathic pains (Siemionow and Brzezicki 2009). Following peripheral axotomy, the dorsal root ganglion (DRG) and ventral horn neurons undergo a series of retrograde degenerative changes ending to neuronal death (Himes and Tessler 1989; Vestergaard et al. 1997; Pierucci and de Oliveira 2006; Johnson et al. 2008). The degenerative changes of neurons occur through damage-induced interruption of the flow of

✉ Mohammad-Amin Abdollahifar
m_amin58@yahoo.com; abdollahima@sbmu.ac.ir

¹ Hearing Disorders Research Center, Loghman Hakim Medical Center, Shahid Beheshti University of Medical Sciences, Tehran, Iran

² Department of Biology and Anatomical Sciences, School of Medicine, Shahid Beheshti University of Medical Sciences, Tehran, Iran

³ Department of Anatomical Sciences, Lorestan University of Medical Sciences, Khorramabad, Iran

⁴ Department of Anatomical Sciences, School of Medicine, Sabzevar University of Medical Sciences, Sabzevar, Iran

⁵ Department of Anatomy and Neuroscience, faculty of Medicine, Dentistry and Health Science, University of Melbourne, Melbourne, VIC, Australia

neurotrophic factors from perimeter to neuronal body by retrograde transport (Johnson et al. 2008). Nevertheless, researchers have utilized three different types of graft including allografts, auto-grafts, and xenografts to regenerate nerves; all three types, however, have the following disadvantages: immunological rejection and finite availability (Terenghi 1999; Hyun and Kim 2010). Until now, no efficient approach has been found for better regeneration of the neural tissue; it is thus necessary to develop artificial nerve grafts. ECM-like structures have been investigated as an ideal scaffold for neural tissues regeneration and repair. In particular, the aligned nanofibers have proven to be more suitable for neurite development compared with the haphazardly oriented nanofibers, because this alignment establishes guidance cue given that anatomical properties of normal nerves have been extremely structured and aligned (Zalewski and Gulati 1981; Lee et al. 2005). Poly ϵ -caprolactone (PCL) is a semi crystalline linear hydrophobic polymer. Although electrospun PCL mats mimic the identity of ECM in the living tissues, its weak hydrophilicity reduces capability of the cell adhesion, emigration, differentiation, and rapid growth (Kim et al. 2006; Schnell et al. 2007). In other words, the natural biomolecules obtained from biological origins possess excellent biocompatibility and have a widespread utilization in medication and medical areas (Li et al. 2006; Chong et al. 2007).

One of the components of fibrinolytic mechanism is tissue plasminogen activator (tPA) classified as a serine protease converting zymogen plasminogen into the active protease plasmin (Koh et al. 2008). Notably, this proteolytic cascade is capable of degrading fibrin and the remaining extracellular matrix proteins (Vassalli et al. 1991). In fact, tPA is predominantly present in the blood though it is found in other systems, too. On the one hand, tPA is basically generated in the central nervous system (CNS) through neurons and microglia (Mayer 1990; Tsirka et al. 1995). Moreover, its diverse performances in motor learning, lengthy potentiation, and seizure have been reported in various studies. On the other hand, it would mediate excitotoxic neurodegeneration via cleaving plasminogen into plasmin and starting a proteolytic cascade, resulting in neuronal death (Qian et al. 1993; Seeds et al. 1995). In peripheral nervous system (PNS), tPA is quickly produced in the sensory neurons and Schwann cells after sciatic nerve injury (Tsirka et al. 1997; Mataga et al. 2002; Yepes et al. 2002). Basically, rats with no tPA or plg genes exhibited greater level of axonal degeneration, myelin sheath decomposition and hindered functional recoveries after the sciatic nerve damage (García-Rocha et al. 1994; Siconolfi and Seeds 2001). According to the previous researches, tPA/plg system can contribute to degenerating and regenerating the peripheral nerves when an injury occurs. Even though the absence of tPA hinders the recovery of the nerves following an injury, there is not enough knowledge of how exogenous tPA or tPA/plg affects the nerve regeneration following an injury.

Accordingly, the current study aims to evaluate the post-axotomy effects of tPA containing structure on the sciatic nerve, DRG, and anterior horn of spinal cord in male rat.

Material and Methods

Materials and Fabrication Method

Polycaprolactone and tissue plasminogen activator (tPA) have been bought from Sigma Aldrich. Moreover, Merck has been chosen to buy Formic acid, Acetic acid, and glutaraldehyde (Germany). Polycaprolactone nanofibrous mat has been made by electrospinning procedure. To sum up, 15 wt% polycaprolactone solution was prepared in a specific solvent system containing acetic acid/formic acid (8:2 ratio) and following the overnight shaking, the procured polymer solution has been placed in a 5 mL glass syringe and then loaded in the syringe pump of the electrospinning mechanism. It is notable that electrospinning has been run towards a rotating mandrel. At the second step, tPA was coated on the nanofibers using plasma treatment. Briefly, tPA have been swollen in 0.05 M acetic acid at 4 °C overnight for producing a 0.1% (w/v) suspension and the final suspension has been homogenized. Electrospinning was performed with an applied voltage of 22 kV, flow rate of 0.8 mL/h and the spinneret/collector distance of 15 cm. It is notable that electrospinning has been run towards a rotating mandrel of 200 rpm. The concentration of the tPA in the suspension has been reported in the text as 0.1% (w/v). Electrospun mat was located in the plasma chamber at 50 w power and 500 mTorr pressure. The surfaces of strands were treated by Argon discharge plasma for 240 min. Immediately after plasma treatment, prepared tPA suspension was added to the mat and treated samples were allowed to react overnight at 4 °C. Finally, tPA-coated mats were cut into 1.4 × 2 cm specimens to be wrapped around the 1-cm nerve gap site by fixing on its distal and proximal parts. Samples were sterilized by UV radiation prior to being used for in vitro and in vivo experiments.

Released tPA Activity from the PCL Scaffold over Time In Vitro

Serine protease converts plasminogen into plasmin, which subsequently digests the chromogenic substrate to a color product with a maximum absorbance at 405 nm. Release behavior of tPA-loaded PCL scaffold in vitro was carried out at 37 °C in 10 mL of 0.1 M PBS (pH = 7.4). The release medium was withdrawn at pre-determined time intervals, and replaced with a fresh soaking medium each time. Then, the concentrations of tPA were determined by UV spectrophotometer by measuring the maximum absorbance at the 405 nm. The concentration of tPA was calculated with a calibration curve from

tPA standard solutions at different concentrations. According to the results, a slight burst release occurred of the total loaded tPA from the PCL scaffold after 3 to 18 days interval. The tPA release from PCL scaffold became quite slow after 21 days (Soleimani et al. 2007) (Table 1 and Fig. 1).

Scanning Electron Microscope Observations

According to the research design, morphological description of the resulting structure was performed with Scanning Electron Microscope (VEGA, SEM, & TESCAN, Czech). In addition, average diameters of the electrospun fibers have been estimated via measurement of 25 fibers in each specimen from the SEM micrographs with the help of the image analysis software (Image JTM, NIH, MD, USA).

Testing the Water Uptake

Notably, the water uptake capacity of the procured samples has been estimated via soaking them ($n = 3$) in the phosphate-buffered saline (pH of 7.4) at 37 °C for 0.5, 1, 6, and 24 h. Moreover, the ratio of the weight enhancement ($w_w - w_d$) to the initial weight (w_d) defines the water to uptake ratio. Here w_w refers to the scaffold weight after immersion in the PBS solution at each time. w_d represents initial weight of the dries scaffold. Moreover, values are written as the means \pm standard deviation (SD).

Contact Angle Measurement

Surface wettability is an important property because of its impacts on the cellular behavior like their viability, bonding, rapid growth and migration. Moreover, for measuring the surface hydrophilicity of the procured structures, water contact

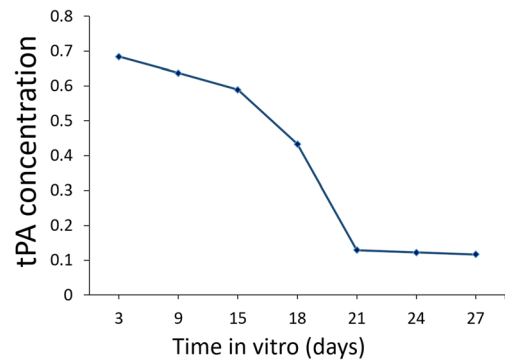


Fig. 1 Released tPA activity from the PCL scaffold in vitro at different time. The concentrations of tPA were determined by UV spectrophotometer by measuring the maximum absorbance at the 405 nm. The results showed that a slight burst release occurred of the total loaded tPA from the PCL scaffold after 3 to 18 days interval. The tPA release from PCL scaffold became quite slow after 21 days

angle analysis was done using sessile drop technique (KRUSS G10, GERMANY).

In Vitro Evaluation

L929 Cell Culture

The present research utilized L929 mouse fibroblast cell line to do in vitro assays. Therefore, the cells have been cultured in RPMI 1640 medium containing 10%FBS, 1% penicillin/streptomycin, and, 1% L-glutamine in the T-75 flask tissues culture. Then, the cells between four and six passages have been exploited in the tests. Afterwards, they have been kept at 37 °C, 5% CO₂, and 95% air. This culture medium has been refreshed every 3 days. Of course, at confluence, the fibroblast cells have been harvested, then, they sub cultivated in a similar medium. Finally, 0.05% trypsin/EDTA has been used for

Table 1 Tissue plasminogen activator (tPA) activity and release behavior in vitro

Sample	tPA activity (IU/mL)	A ₄₀₅
tPA standard		
Undiluted	0	0.02
1:4	0.5	0.23
2:4	1.0	0.44
3:4	1.5	0.62
4:4	2.0	0.84
Tissue plasminogen activator loaded PCL nanofibrous scaffold		
3 days	1.54	0.68
9 days	1.49	0.65
15 days	1.37	0.58
18 days	1.00	0.46
21 days	0.26	0.13
24 days	0.24	0.12
27 days	0.22	0.115

dissonication of the cells, and thus the cells have been centrifuged and re-suspended in the medium before to use.

Cytotoxicity Test

According to the research design, indirect cytotoxicity experiments using L929 mouse fibroblast cell line have been used to examine probable releasing the lower molecular weight cytotoxic materials from the samples. In order to achieve the extracts, sterilized samples have been submerged in the DMEM medium complemented with 1% penicillin/streptomycin and 10% fetal bovine serum (FBS). Moreover, the non-interfered complete medium has been regarded for preparing the controls. In addition, 24 h prior to the addition of the extracts, L929 cells have been seeded (cell density = 2×10^4 cells/well) in the 96-well tissue culture plate. Following incubating for 1 and 4 days, the extracts and the non-interfered media have been removed, then replaced with the medium of the preseeded cells. Of course, 3 replicates have been regarded for all eluates and media. When 24 h passed, 3-(4,5-dimethylthiazol-2-yl)-2,5-diphenyl-2H-tetrazolium bromide (MTT) salt was added to each well and incubation of the plate continued for 4 h. Then, 100 μ l from the solution of each of the wells has been transported to a 96-well plate and adsorbance in the wavelength of 490 nm has been gauged by the Thermo Scientific Multiscan Spectrum plate reader. Results have been provided as the relative ratio of sample values to the control ones.

In Vivo Evaluations

Animals

In this study, twenty-four adult male rats were used. Each rat has been stored in a lab with the standard conditions at 22–24 °C receiving necessary water and food freely. Moreover, the approval of the animals experiment has been received from the Ethics Committee of the Shahid Beheshti University of Medical Sciences (IR.SBMU.RETECH.REC.1396.544). The rats have been categorized into four groups; Group I (Control group): The animals of this group were intact. Group II (axotomy): The rats whose skin and fascia of the posterior thigh were opened and sciatic nerve cut in the midpoint (10 mm piece of the nerve has been removed), Group III (Scaffold): In this group the sciatic nerve was cut, and scaffold free tPA has been interposed into this nerve gap (10 mm). Group IV (tPA-loaded scaffold): In this group, the sciatic nerve was cut, and tPA-coated structure has been interposed into this nerve gap (10 mm).

Surgical and Transplantation Procedures

According to the research design, the animals have been anesthetized and their skins have been incised. Then, a muscle

splitting incision has been used to expose the sciatic nerve. Afterwards, using an operating microscope, the left sciatic nerve has been exposed at the mid-thigh, and a 10 mm piece of the nerve has been removed. In addition, a 14 mm mat has been interposed into the prepared nerve gap and wrapped. Moreover, the two proximal and distal ends of the nerve have been fixed to scaffold by epineurial suture and at the final stage of the surgical operation, skins and fascia have been sutured with 3–0 nylon thread. Finally, al oxytetracycline spray has been used to the infection prophylaxis for 7 days following the surgical operation.

Sciatic Function Index

The sciatic functional index (SFI) has been used to express the functional evaluation of the sciatic nerve regeneration. Four, eight and 12 weeks' post-surgery, walking pattern of animals have been registered to analyze SFI. Briefly, the rats were trained a few pre-experiment for walking down a wooden track (100 \times 20 \times 15 cm) into the darkened goal box. When the surgical operation ended, the animal's hind paws have been dipped using inkpad and alterations in the paw prints originating from the nerve lesion and denervation have been registered. Then, recording proceeded till 5 measurable footprints have been obtained. According to the footprints, these variables have been calculated using a ruler: the print length (PL), which refers to the distance between the heel to the top of the 3rd toe, intermediary toe spread (ITS), which refers to the distance between the 2nd to the 4th toe and toe spread (TS) the distance between the first and the fifth toe. In addition, each measurement has been obtained both through the right experimental foot (EPL, ETS and EITS, respectively) as well as from the left non-operated foot (NPL, NTS and NITS, respectively) of each animal. However, using the above information, the SFI was calculated by the equation below (Varejão et al. 2004):

$$\text{SFI} = -38.3 (\text{EPL}-\text{NPL})/\text{NPL} + 109.5 (\text{ETS}-\text{NTS})/\text{NTS} + 13.3 (\text{EIT}-\text{NIT})/\text{NIT}-8.8$$

The SFI value of nearly 0 represents normal, while an SFI value of -100 indicates total abnormality of the sciatic nerve.

Preparing the Tissue

According to the research design, animals have been deeply anesthetized and decapitated. In the next stage, their DRG, right sciatic nerve, and spinal cord have been immersed in 10% formaldehyde for 1 week and after this time it included in the paraffin block. Then, thin sections (5 μ m) and thick section (25 μ m) have been incised by means of a microtome

and eosin, hematoxylin, Luxol fast blue, cresyl violet, and osmic acid have been used to stain them.

Stereological Study

Total Number of the Nerve Fibers

A two-dimensional fractionator's procedure has been used to estimate total numbers of the nerve fibers. Moving the microscope stage in x and y directions has been shown by 2 dial gauges. Then, an un-biased counting frame has been superimposed on the cross-section of the sciatic nerve (Larsen 1998). The total number of nerve fibers has been determined by the formula provided below:

$$N = \frac{1}{\text{sf}} \times Q$$

$$\text{sf} = \frac{a(\text{frame})}{a(\text{sample})}$$

Here, sf refers to the sample fraction. $a(\text{frame})$ stands for the area per frame. $a(\text{sample})$ is the sampling area. Q represents the number of the nerve fibers.

The Diameter of the Nerve Fiber

The nerve fiber diameter has been determined on the nerve fiber, which has been taken sample via the counting frame. Moreover, the widest line passing nearly across the central point of the nerve fiber and vertical to the longest axis of the nerve fiber has been regarded as the diameter. In addition, two-dimensional nucleator technique has been utilized for estimating the fibers cross-sectional areas (Jensen et al. 1979; Karlsson and Cruz-Orive 1997). With regard to the approximated central point of the nerve fiber, the length of both test lines (perpendicular to each other) from the center to the nerve fiber boundary, L_n , has been measured. Then, the area has been determined by this formula:

$$D = \frac{\pi}{4} \times L_n$$

In this formula, the L_n is the mean of the length of both test lines.

Estimating the Myelin Sheath Thickness

A systematic, IUR sample of the sites to directly measure the thickness of myelin sheath has been obtained by means of the intersection points between the axon perimeter and the test lines employed to estimate the perimeter estimation. It should be noted that orthogonal thickness (t) of the myelin sheath for all axons has been approximated as the average of 4 measurements. Then, the intersection points have been numbered

consecutively so that the first position has been selected randomly in the first 1/4 interval, the 2nd position has been 1/4 position 1, the 3rd position has been 1/4 position 2, and the 4th position has been 1/4 position 3.

$$T = \frac{\pi}{4} \times L_n$$

In this formula, the L_n is the means of the intersection points between the axon perimeter and the test lines.

Estimation of the Volume of Dorsal Root Ganglion and the Anterior Horn of the Spinal Cord

Cavalier's procedure has been used for estimating the size or volume of ganglion by means of this formula:

$$V_{\text{total}} = \sum P \times \frac{a}{p} \times t$$

Here " V " refers to ganglion volume. " $\sum P$ " is the total numbers of the points that hit the compartment in the chosen sections. " t " stands for the distance between the sections and " a/p " represents the area per point (Noorafshan et al. 2011; Noorafshan et al. 2012).

Mean Volume of Anterior Horn Neurons and Sensory Neurons of DRG

According to the research design, a nucleator procedure estimates the volume. Then, spinal cord samples have been inserted in a paraffin block, cut in sections of 25 μm in thickness, and then cresyl violet has been used to stain them. In the next stage, the optical disector has been used to sample the neurons. In fact, for all sampled nucleolus, 2 horizontal directions (intercept, L_n) have been viewed from the central point into the nucleolus to the cell or nucleus borders (Fig. 3). Then, according to a set of the above measurements (120 intercepts in each group), estimation of the mean nucleus and the cell volume in the number weighted distribution have been done by the following relation (Gundersen et al. 1988a; Gundersen et al. 1988b):

$$V_n = \frac{4\pi}{3} \times L_n$$

Estimating the Number of the Neurons, Satellite Cells of DRG, and Number of Neuron and Glial Cell of the Anterior Horn of the Spinal Cord

An optical disector procedure has been used to determine total numbers of the neuron, glial cells and satellite cells. Then, an equal interval of the movement stage and systematic uniform random sampling has been used to select the

microscopic field position (Gundersen et al. 1988a, Gundersen et al. 1988b).

According to the research design, a microcator has been utilized to measure the Z-axis movement of the microscope phase. Moreover, an un-biased counting frame containing the exclusion and inclusion boundaries has been superimposed on the sections images observed on the monitor. In addition, a nucleus has been counted in a case of complete or partial placement into the counting frame and when it has been not close to the exclusion line. The formula provided below has been used to calculate the numerical density (N_v):

$$N_v = \frac{\Sigma Q}{\Sigma P \times h \times \frac{a}{f}} \times \frac{t}{BA}$$

Here ΣQ refers to the numbers of nuclei, h is the dissector height, a/f represents the frame area, and ΣP indicates total numbers of the un-biased counting frame in each field. Moreover, t refers to real thickness of the section gauged in all fields with a microcator. In addition, BA stands for the microtome block advance that has been adjusted at 10 μm . Finally, total numbers of neuron and satellite cells have been determined via multiplication of the numerical density (N_v) by the total volume.

$$N_{\text{total}} = N_v \times V_{\text{total}}$$

Immunohistochemical Study of GFAP Expression in Anterior Horn of the Spinal Cord

Immunohistochemical staining is used for analysis of expression of GFAP that is one of the astrocyte markers in segments of the anterior horn of spinal cord. Firstly, we de-paraffinized the tissue section slides in xylene (Merck: Germany). Then, these slides have been immersed in ethanol (Merck, Germany) in order to rehydrate. In the next stage, we transported the tissue slides into 10 mM sodium citrate buffer (Sigma, St. Louis, MO, USA) at pH 6.0 in order to Antigen retrieval. The tissues were incubated in 3% hydrogen peroxide in the room temperature for 10 min for blocking the endogenous peroxidase activities. Between incubation, 2 washes have been done with Tris/HCl buffer (Sigma; St. Louis; MO: USA) at pH equal to 6.0. Incubation of the sections has been then performed in polyclonal rabbit anti-GFAP (1:250; PA1-10019; Invitrogen; Waltham, MA USA), immunoglobulin as the primary antibody for 16 h followed by a biotinylated secondary antibody (Invitrogen; Waltham, MA USA) based on the company guidelines. Visualization of immune reactivity has been observed following the tissue sections incubation in diaminobenzidine solution 0.1% (Sigma, St. Louis, MO, USA). At the end, we counterstained the solution with the Harris' modified hematoxylin (Sigma, St. Louis, MO, USA) solution.

Real-Time Quantitative RT-PCR

It is notable that qRT-PCR has been chosen to analyze level of S100, NGF, and BDNF expression. Moreover, the total RNA has been derived from tissue samples by means of Trizol reagent according to the company guidelines (add 1 mL TRIZol for 50~100 mg tissue, homogenize on ice with a mechanical homogenizer, and incubate on ice for 5 min). Therefore, cDNA has been synthesized according to the total RNA via a Prime Script RT reagent kit with gDNA Eraser (Takara: Dalian). Of course, for reverse transcription polymerase chain reaction (RT-PCR), the PCR reaction involved 35 cycles of denaturation at 94 °C for 30 s, extension at 72 °C for 30 s, and annealing at 54 °C for 3 s. In addition, PCR products for S100, NGF, and BDNF respectively have been 109, 195, and 182 bp. Table 2 presents the primers. In order to run the real-time quantitative RT-PCR, we utilized Fast Start Universal SYBR Green Master (Roche: US) over a Master cycler ep realplex 4 system (Eppendorf: German) to accomplish the processes. Each reaction has been done three times. Finally, the comparative $2^{-\Delta\Delta C_t}$ procedure has been used to calculate mRNAs relative expression and then data normalized versus GAPDH (Table 2).

Statistical Analysis

Data have been written as the mean \pm SD. Notably, SPSS17.0 (Chicago: USA) has been used to analyze the obtained data. Moreover, the statistical significance has been determined by means of one-way ANOVA and Kruskal-Wallis to compare the data obtained. In addition, significance level has been considered $P < 0.05$.

Result

Scaffold Morphology

SEM micrographs of the prepared structures are shown in Fig. 2. Nanofibrous microstructure can be seen in these images (Fig. 2). Incorporation of tPA on the fibers are clearly observable in Fig. 2b. According to the results, plasma treatment following by tPA coating have not any worse effect on the microstructure of the prepared samples and by formation of a thin layer on the fibers, a large surface area of tPA would be introduced for the regenerating axons.

Testing the Water Uptake

Figure 3 is a report of the capacity of the water uptake of the procured samples. Accordingly, the applied modification by plasma irradiation and tPA coating, resulted in the proper

Table 2 Primer design

Genes	Primer sequences	Product size (base pair)	TM
GAPDH	F = ATCACTGCCACTCAGAAGACTG R = TGGATGCAGGGATGATGTTCTG	293 bp	60 °C
BDNF	F = GTAGTTTTTCGTAGGATGAGGAAGC R = AATATAAATTAACAACCCCGATACG	253 bp	60 °C
NGF	F = TGC ATA GCG TAA TGT CCA TGTTG R = CTG TGT CAA GGG AAT GCT GAA	205 bp	59 °C
S100	F = ACT GAA GGA GCTATCAACAACGA R = AGT GTG ACT TCC AGG AGT TCATG	205 bp	60 °C

water uptake capacity of the structure. In addition, a remarkable value in the water uptake capacity of the tPA-coated structure was detected from the first minutes of the test compared with that of unmodified structure.

Contact Angle

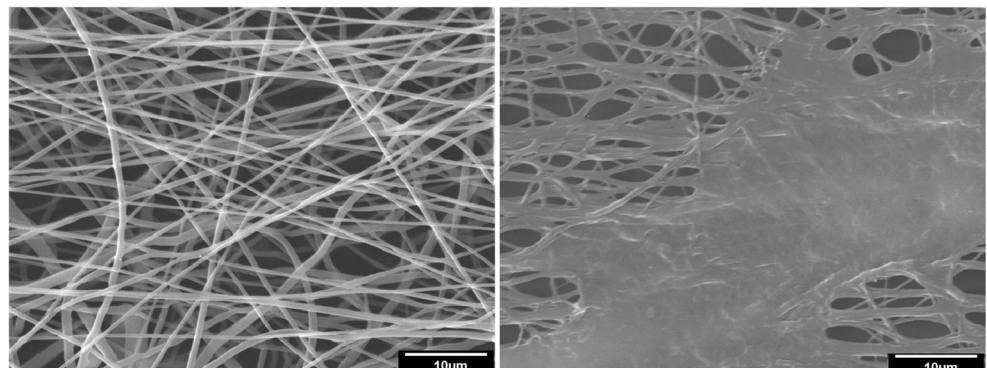
Water contact angle measured on the surface of the prepared structures is summarized in Table 3 as a function of time. According to the results, plasma treatment followed by the coating of tPA enhanced the wettability of the nanofibrous surface so that the water contact angle on the tPA-coated surface approached to zero which indicates that water drop was immediately absorbed into the structure. Accordingly, it can be concluded that the prepared structure is hydrophilic and can be used successfully in vivo environments and appropriate cell behavior would be guaranteed.

Water contact angle on the surface of prepared samples (Table 3).

In Vitro Cytotoxicity Evaluation

Probability of the release of cytotoxic materials from the prepared samples has been examined via indirect cytotoxicity test using L929 mouse fibroblast cell line and MTT assay. Obtained results indicated the complete viability of cells at the exposure with both tPA-free and tPA-loaded samples (Fig. 4).

Fig. 2 SEM micrograph of the nanofibrous surface before and after tPA loading



Sciatic Function Index

Figure 5 A–C show SFI values in the experimental group. SFI was performed every 4 weeks over 12 weeks' post-surgery. After 12 weeks, rats with scaffold and tPA-loaded scaffold had significantly less motor impairment when compared with those with axotomy group ($P < 0.05$, $P < 0.01$) respectively (Fig. 5C). Our results showed that the rats with tPA-loaded scaffold were significantly improved from week 12. Interestingly, there was a statistically significant difference between scaffold and tPA-loaded scaffold groups at week 12 ($P < 0.05$) (Fig. 5C). The SFI-values at week 4 and 8 was not significantly different between axotomy group with scaffold and tPA-loaded scaffold groups (Fig. 5C). Following the nerve transection, the mean SFI value declined to -60 because of significantly less motor function in the axotomy rats. Upon the completion of the research, scaffold group and tPA-loaded scaffold group showed the mean value for SFI of -35.3 and -23.5 respectively, while the mean value of -14.2 has been observed in the controls. Moreover, data have been statistically analyzed showed that administration of tPA-free and tPA-loaded scaffolds enhanced the functional recoveries over time (Fig. 5A–C).

Total Number of the Nerve Fiber, Thickness of Myelin Sheath, and High Magnifications of Sciatic Nerves 12 Weeks Post-Surgery

In osmic acid staining, normal nerve presented morphologies of regular nerve fiber alignment and normal sciatic nerve had

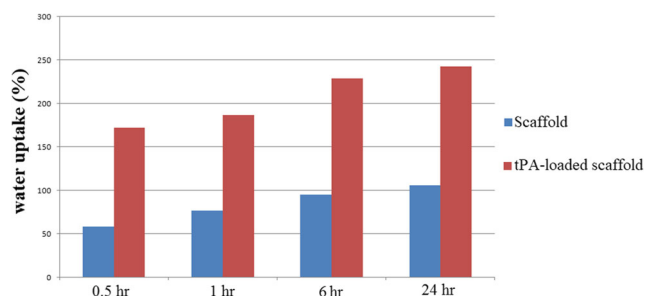


Fig. 3 Water uptake behavior of structures in PBS solution up to 24 h

dense myelinated nerve fibers with comparatively uniform size and large diameter (Fig. 6A–G). The results revealed total number of nerve fiber and myelin sheath thickness were significantly reduction in the axotomy groups in comparison to the scaffold ($P < 0.01$), tPA-loaded scaffold ($P < 0.01$) and control ($P < 0.001$) groups (Fig. 6 F and G). Figure 6A–G show the osmic acid images along the cross-sections incised from the segment of the regenerative nerve fibers in different groups following 12 weeks' post-surgery. Actually, the nerves recovered from the scaffold and tPA-loaded scaffold groups showed the enhanced numbers of the nerve fibers and also increasing the myelin sheath thickness. However, the nerve regenerative was observed in the scaffold and tPA-loaded scaffold groups. These findings were also confirmed with osmic acid staining (Fig. 6) and showed higher remyelination in a group transplanted with scaffold and tPA-loaded scaffold.

Total Volume of the Sciatic Nerve

Our results of this study revealed that the total volume of sciatic nerve were significantly reduction in the axotomy groups in comparison to the scaffold group ($P < 0.05$), tPA-loaded scaffold ($P < 0.05$) and control groups ($P < 0.01$) (Fig. 7F). However, the nerve regenerative was observed in the scaffold and tPA-loaded scaffold groups. Interestingly, there were no statistically significant differences between scaffold and tPA-loaded scaffold groups, revealing nerve conduits could have effects on preventing volume reduction. These findings were also confirmed with LFB staining and showed improvement in the volume of sciatic nerve in group of transplanted with scaffold and tPA-loaded scaffold (Fig. 7A–F).

Table 3 Water contact angle on the surface of prepared samples

Sample contact angle	tPA-free surface	tPA-loaded surface
θ_1	86.49 ± 7.30	43.45 ± 6.35
θ_2	84.72 ± 8.26	10.08 ± 3.12
θ_3	84.08 ± 10.03	7.54 ± 2.68

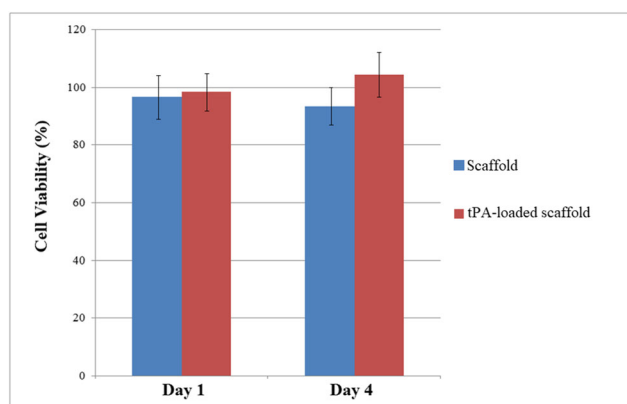


Fig. 4 In vitro cell viability of the prepared samples, using L929 cell line and MTT assay

Total Volumes of the DRG

Based on the results, total volume of the DRG were significantly decreased in the axotomy groups in comparison to the scaffold group ($P < 0.01$), tPA-loaded scaffold ($P < 0.01$), and control groups ($P < 0.01$) (Fig. 8F). Nonetheless, the volume of the DRG was unchanged in the scaffold groups in comparison with the scaffold groups (Fig. 8F). Our finding revealed that using the tPA-loaded scaffold for bridging 10 mm sciatic nerve deficiencies in the animals could prevent reduction in the volume of DRG (Fig. 8F). These findings were also confirmed with H&E staining and showed improvement in the volume of DRG in group of transplanted with scaffold and tPA-loaded scaffold (Fig. 8A–F).

Number of Neuron, Satellite Cells of the DRG

Based on the finding, total numbers of the neurons and satellite cells of the DRG were significant decreased in the axotomy groups in comparison to the scaffold group ($P < 0.05$), tPA-loaded scaffold ($P < 0.01$) and control groups ($P < 0.001$) (Fig. 9 F and G). Interestingly, the total number of neurons in group of tPA-loaded scaffold was significantly differences with scaffold groups ($P < 0.05$) (Fig. 9F). Nonetheless, the total number of satellite cells of the DRG unchanged in the scaffold groups in comparison to the tPA-loaded scaffold groups (Fig. 9 F and G). Our finding of H&E staining revealed that using the tPA-loaded scaffold for bridging 10 mm sciatic nerve deficiencies in the animals could prevent reduction in the number of neuron and satellite cells of DRG (Fig. 9A–G).

Number of Motoneuron, Neuroglial, and Volume of the Anterior Horn in Spinal Cord

Assessing the anterior horn segments of the spinal cord demonstrated remarkably the decreased number of motoneurons

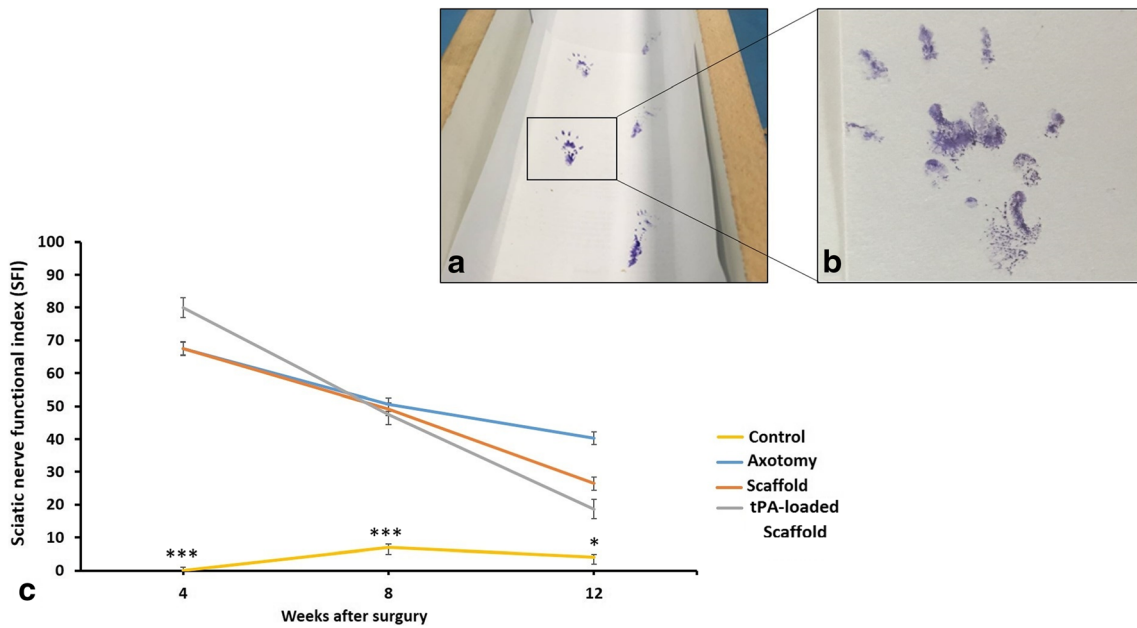


Fig. 5 A, B After 4, 8, and 12 weeks of surgery procedure, image shows the footprint. C The sciatic functional index of different weeks (4, 8, and 12) in the different groups is shown. The significant difference between

control groups with the other groups is indicated. $***P < 0.001$. The significant difference between axotomy groups with the tPA-loaded scaffold groups is indicated. $*P < 0.05$

in the axotomy groups in comparison with scaffold ($P < 0.05$), tPA-loaded scaffold ($P < 0.01$) and control groups ($P < 0.001$) (Fig. 10E). According to the analysis, number of neuroglial cells increase in the axotomized rats in comparison with the tPA-loaded scaffold ($P < 0.05$) and control groups ($P < 0.001$)

(Fig. 10F). Nonetheless, there is no significant different between axotomy groups and scaffold group (Fig. 10F). Based our results, total volumes of anterior horn has been decreased in the axotomized rats in comparison with control groups ($P < 0.01$) (Fig. 10G), but, there is no significant different

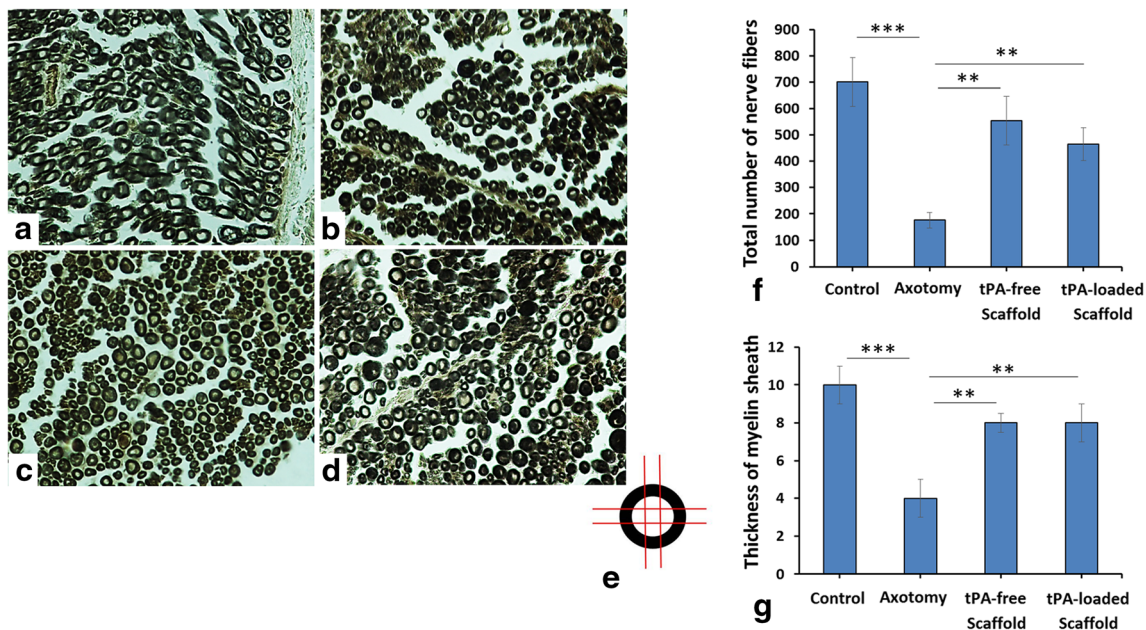
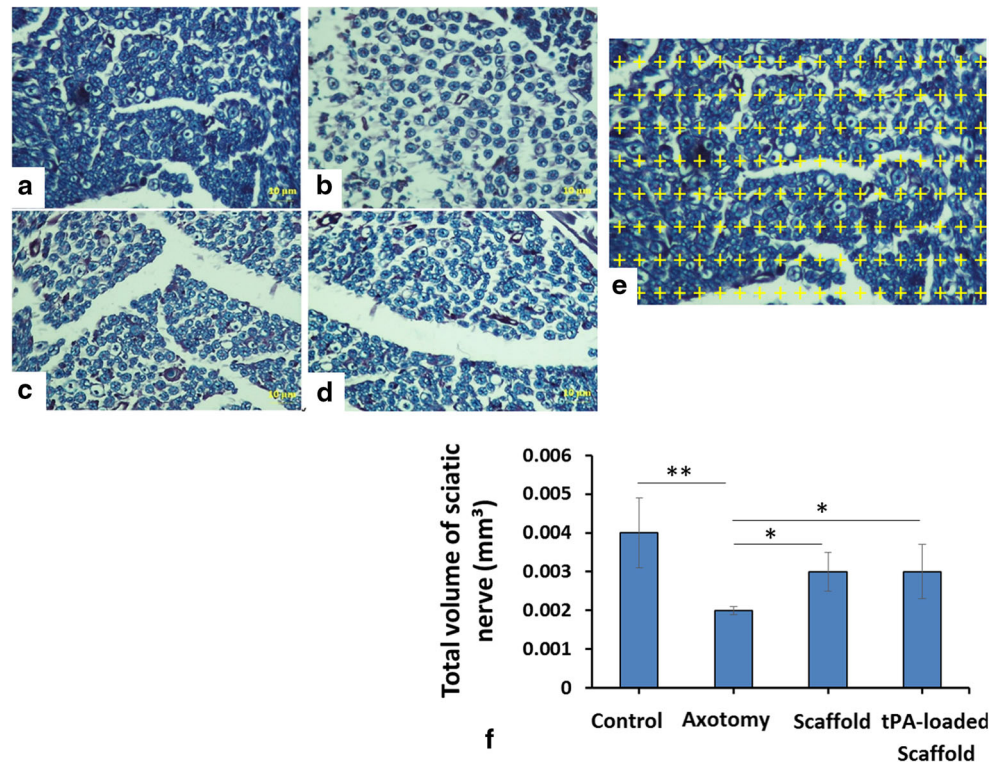


Fig. 6 A–D Micrograph of the sciatic with tetroxide osmium; A control group, B axotomy group, C scaffold group, D tPA-loaded scaffold group. D, E Orthogonal intercepts probe for estimation of myelin sheath thickness. F Total number of nerve fiber: in control, control, axotomy, scaffold, and tPA-loaded scaffold groups. The significant difference between controls with the other groups is indicated. The significant difference

between axotomy with the other groups is indicated ($**P < 0.01$, $***P < 0.001$). G The thickness of myelin sheath: in control, axotomy, scaffolds groups. The significant difference between control with the other groups is indicated. The significant difference between axotomy with the other groups is indicated ($**P < 0.01$, $***P < 0.001$)

Fig. 7 A–D Micrograph of the sciatic nerve stained with Luxol fast blue (LFB); A control group, B axotomy group, C scaffold group, D tPA-loaded scaffold group. E A grid of points was superimposed on the image for estimation of total volume of sciatic nerve. F Total volume of sciatic nerve: in control, axotomy, scaffolds, and tPA-loaded scaffold groups. The significant difference between control with the other groups is indicated. The significant difference between axotomy with the other groups is indicated. (* $P < 0.05$, ** $P < 0.01$)



between axotomy group compare to the tPA-loaded scaffold and scaffold group (Fig. 10F). The data revealed that using the tPA-loaded scaffold for bridging the sciatic nerve deficiencies in the animals could stop the neuron loss, gliosis in anterior horn of the spinal cord (Fig. 10A–G).

The Expression Level of Astrocytic Marker GFAP

Our results showed the increased expression level of the astrocytic marker GFAP in the anterior horn of the spinal cord in the axotomy groups in comparison with the

Fig. 8 A–D Micrograph of the sciatic nerve and DRG stained with hematoxylin and eosin (H&E); A control group, B axotomy group, C scaffold group, D tPA-loaded scaffold group. E A grid of points was superimposed on the image for estimation of total volume of DRG. F The volume of DRG in control, sham, and scaffold groups. The significant difference between shams with the control groups is indicated (** $P < 0.01$)

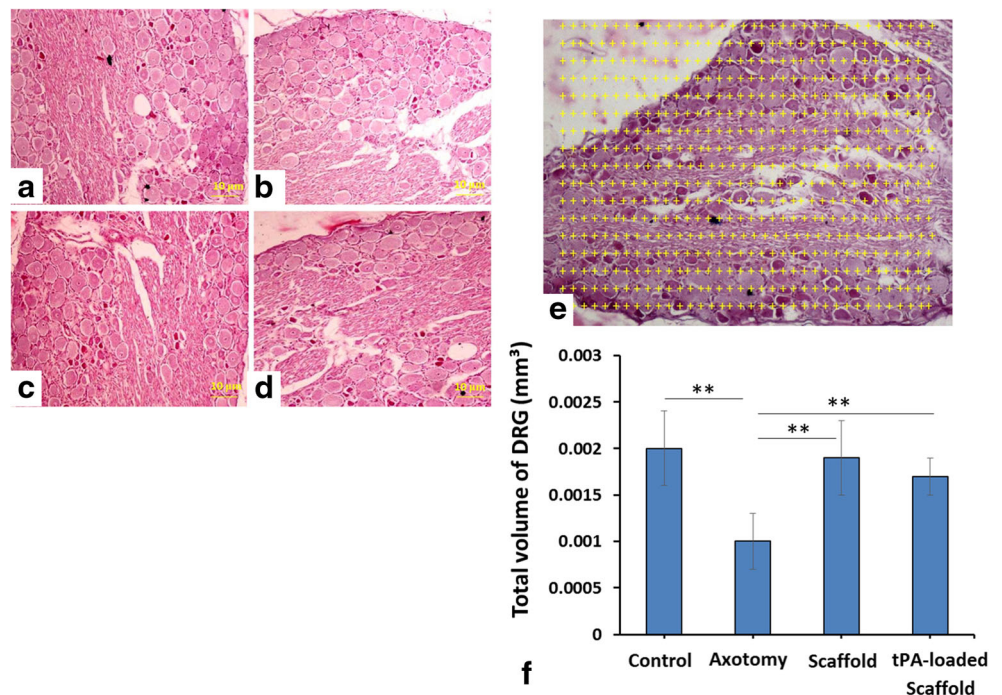
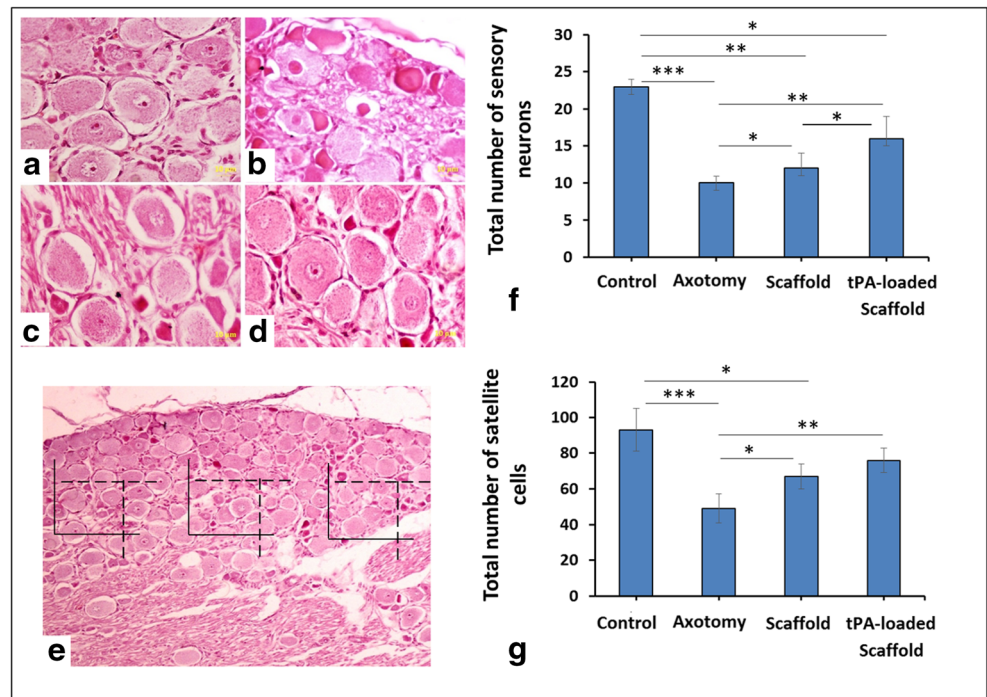


Fig. 9 A Micrograph of the sciatic nerve and DRG stained with hematoxylin and eosin (H&E); A control group, B axotomy group, C scaffold group, D tPA-loaded scaffold group. E Counting frames were superimposed on images for estimation of total number of sensory neurons in DRG. F The total number of sensory neuron in control, sham, scaffolds, and tPA-loaded scaffold groups. The significant difference between shams with the other groups is indicated (* $P < 0.05$; ** $P < 0.01$; *** $P < 0.001$). G The number of the satellite cell in DRG remained unchanged in the sham in comparison with the other groups (* $P < 0.05$; ** $P < 0.01$; *** $P < 0.001$)



scaffold group ($P < 0.05$), tPA-loaded scaffold ($P < 0.01$), and control groups ($P < 0.001$) (Fig. 11E). Our results also showed that the GFAP positive cells significantly increased in the scaffold group compare to the tPA-loaded scaffold ($P < 0.05$) and control group ($P < 0.01$)

(Fig. 11E). However, these findings of immunohistochemistry of astrocytic marker were also confirmed the astrogliosis was observed in the axotomy groups in comparison to the tPA-loaded scaffold, scaffold group and control groups (Fig. 11A–D).

Fig. 10 A–D Photomicrograph of the spinal cord stained with cresyl violet. A Control group, B axotomy group, C scaffold group, D tPA-loaded scaffold group. E Total number of motor neurons. F Total number of glial cells. G Total volume of anterior horn in the different groups is shown. The significant difference between control with the axotomy groups is indicated (* $P < 0.05$; ** $P < 0.01$; *** $P < 0.001$)

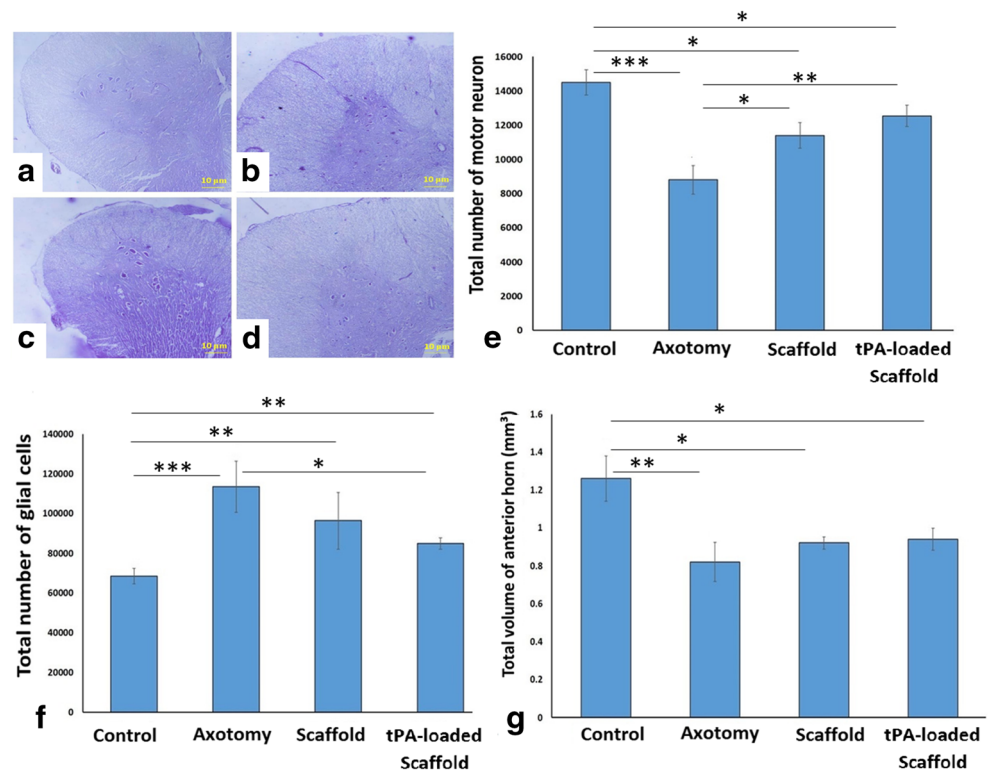
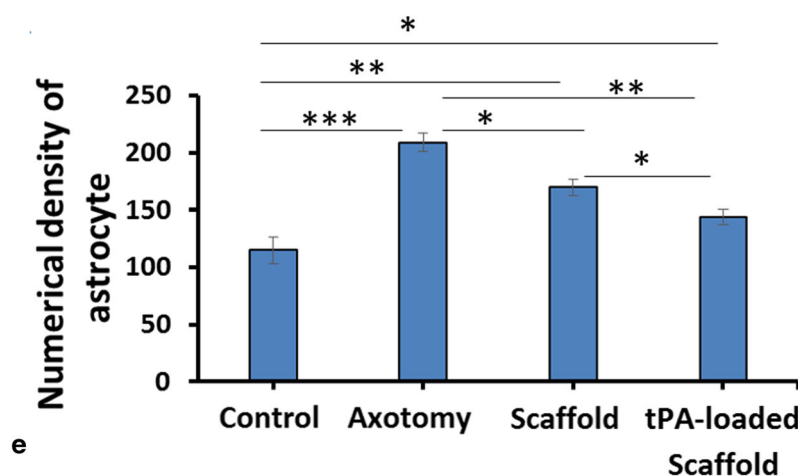
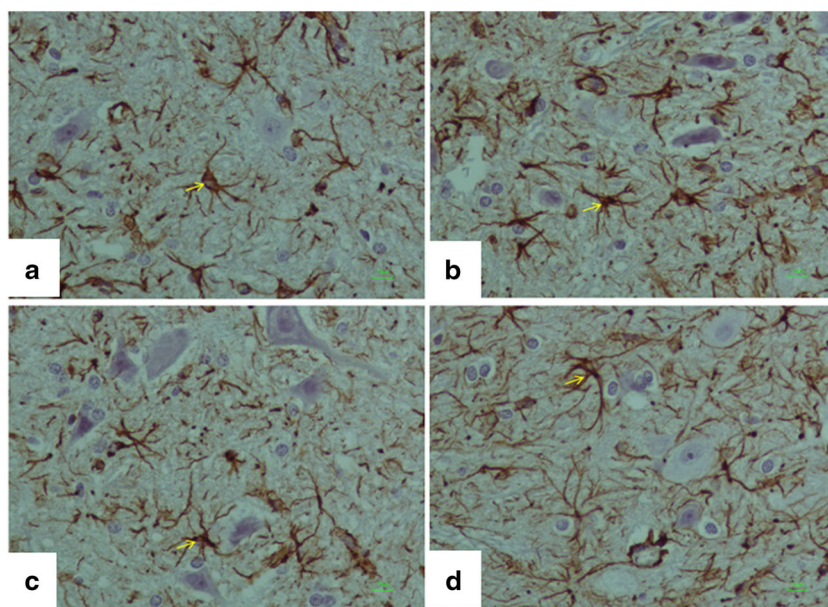


Fig. 11 A–D Astrocytic immunostaining for GFAP in the anterior horn of spinal cord. Astrocyte (yellow arrow). A Control group, B axotomy group, C scaffold group, D tPA-loaded scaffold group. E Representation of the estimated parameters of the anterior horn. Numerical density of GFAP positive cells in anterior horn of spinal cord in the different groups is shown. The significant difference between control with the axotomy groups is indicated (* $P < 0.05$; ** $P < 0.01$; *** $P < 0.001$)



Level of *S100*, *NGF*, and *BDNF* Expression

According to the research of this study, relative expression of mRNA of *S100*, *BDNF*, and *NGF* has been normalized by control between different groups and quantitated. According to Fig. 12A–C, level of *S100* and *BDNF* expressions in the sciatic nerve tissue have been considerably decreased in the axotomy groups in comparison to the scaffold group ($P < 0.001$), tPA-loaded scaffold ($P < 0.001$) and control groups ($P < 0.01$) (Fig. 12 A and C). Our results of level of *NGF* expressions in the sciatic nerve tissue have been considerably decreased in the axotomy groups in comparison to the scaffold group ($P < 0.01$), tPA-loaded scaffold ($P < 0.001$) and control groups ($P < 0.01$) (Fig. 12B). These findings were also indicated that the increasing the expression levels of nerve regenerative biomarkers such as *S100*, *BDNF* and *NGF* in the scaffold and tPA-loaded scaffold groups in comparison to the axotomy groups.

Discussion

After peripheral nerve injury with large gaps, proximal segment of axons may regenerate and distal segment initiate Wallerian degeneration (Frattini et al. 2012). Because of peripheral nerve after injury has the ability for regeneration, using of a nerve auto-graft is a golden standard to repair or fix the nerve deficiencies clinically, these solutions have certain limitations and therefore the use of nerve conduction guides for nerve regeneration can be a therapeutic approach (Ghasemi-Mobarakeh et al. 2008; Yu et al. 2011).

The current research dealt with investigating and utilization of tPA for sciatic nerve repair. The utilization of the biological materials or the synthetic substances such as scaffolds at the site of nerve ending is increasingly considered by researchers. On the other hand, research indicated that the use of scaffolds has an important role in the migration of glial cells, growth of neuritis, and increasing their survival and proliferation. The

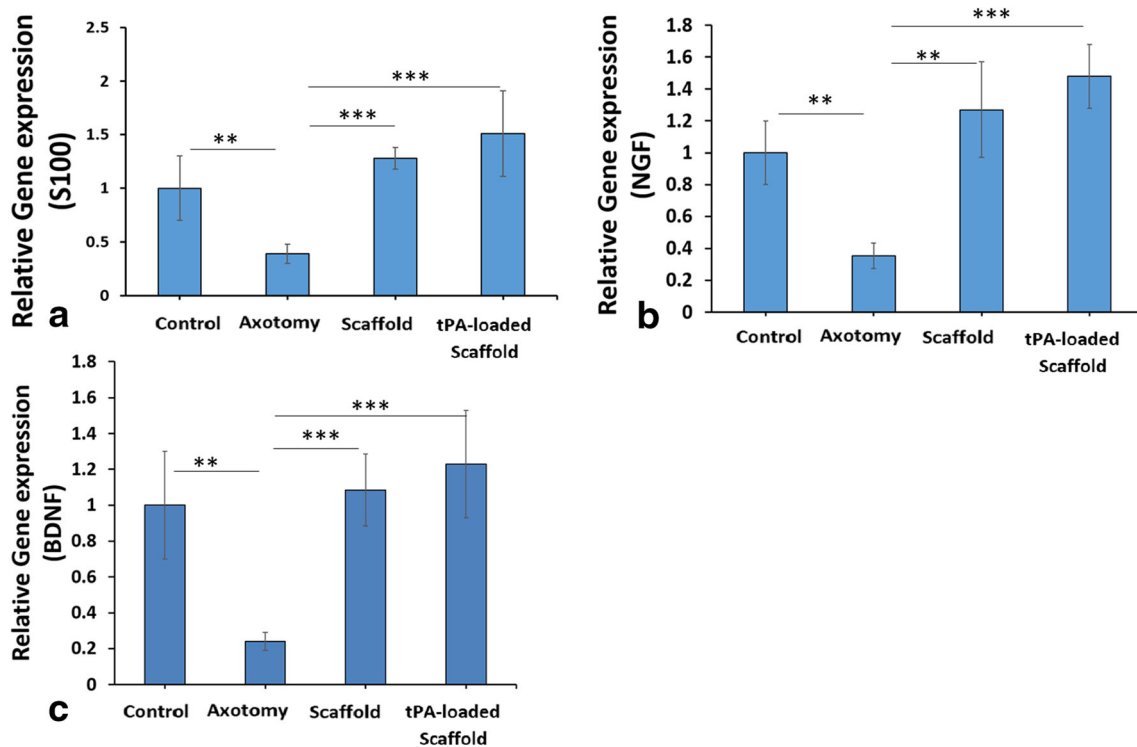


Fig. 12 A–C Real-time PCR; relative gene expression of S100, NGF, and BDNF in control group, axotomy group, scaffold group, and tPA-loaded scaffold group. The significant difference between scaffolds groups with

axotomy is indicated. The significant difference between scaffold group with tPA-loaded scaffold group is indicated (* $P < 0.05$; ** $P < 0.01$; *** $P < 0.001$)

sciatic nerve injury results in loss of relative or complete sensory and motor function (Willerth and Sakiyama-Elbert 2007). The use of artificial scaffolds has been increasingly studied with regard to their ease of access, flexibility and reasonable prices (Prabhakaran et al. 2008). Among these scaffolds, nanofibrous scaffolds provide a space similar to the extracellular matrix for cells by forming a network of permeable fibers with a plurality of pores, which affects the morphology, orientation, adhesion, migration, differentiation and function of the cell (Cao et al. 2009). In the present study *tPA-loaded* scaffold was used to investigate the recovery of sciatic nerve injury as a pattern of peripheral nerve injury. *tPA* loading provided a biocomposite with potentially improved biocompatibility and neural regeneration capability which provide the sustained availability of the surface protein during the regeneration time. Our findings proved that *tPA-loaded* scaffold, could enhance regenerating the sciatic nerve, which has been documented by the higher rate of survival of sensory and motor neuron, and more acceptable recoveries of the motor functions. In vivo findings indicated time-dependent decreases in SFI values due to sciatic nerve degeneration in the axotomy groups compared with the other groups. In this study, we found that transplantation of *tPA-loaded* scaffold could notably increase the numbers of the nerve fibers in SNFs, number of the neurons and glial cells in anterior horn of the spinal cord, numbers of the sensory neurons and satellite cells in the DRG. Likewise, the volume of sciatic nerve,

anterior horn and DRG increases in mice after the transplantation with *tPA-loaded* scaffold. In addition, we also observed a remarkable reduction in astrogliosis, and increase in myelin thickness compared with the axotomy groups, as well as the relative level of mRNA expression of the genes has been examined in sciatic nerve tissues between the population that demonstrated a decline at transcriptional level of S100, NGF, and BDNF in axotomy groups compared with the *tPA-loaded* scaffold groups. Our finding suggests that *tPA-loaded* scaffold may regulate dedifferentiation and proliferation Schwann cell. They undergo changes of secret neurotrophic agents and extracellular matrices and enclose the regenerating axons for forming myelin sheaths that involves providing a desirable environment to regenerate the nerves.

Former research in the field referred to the complete adhesion of the Schwann cells on the electrospun fibers with random alignment, the stretched across several fibers, and the elongated along the fiber axes (Chew et al. 2008). The biomaterials scaffold provide physicochemical markers in accordance with surrounding tissues and provide a specific type of cell for supporting and differentiating tissue engineering applications (Alvarez-Perez et al. 2010). In fact, collagen, which is a major structural protein of ECM, enjoys very good biocompatibility (Yang et al. 2008). According to Yu et al., their electrospun collagen/PCL nerve conduit would enhance neurite extension and axon regrowth. Therefore, it is necessary to use these scaffolds for additional improvement of the

functional regeneration outcomes, in particular for more prolonged restoration of the nerve defects (Böttcher et al. 2009).

According to the already conducted research in the field, tPA is one of the key plasminogen activators induced following the damages to the sciatic nerve (Akassoglou et al. 2000). It has been showed that the tPA-deficient rat showed the worsened degeneration of the nerve and incomplete remyelination following the damages to the nerve (Rogove et al. 1999; Siconolfi and Seeds 2001). The present research determined the impacts of exogenous tPA on regenerating the nerve following the occurred injuries. According to the analyses, the exogenous tPA capable of promoting the axonal regeneration, remyelination, and practical recoveries. In fact, tPA is capable of promoting the nerve regeneration by proteolytic activities and non-proteolytic function. Therefore, it has been speculated that clearing fibrin following the tPA treatment depended on the proteolytic activities and actuation of MMP-9. Therefore, expressing MMP-9 in the macrophages can be dependent on tPA non-proteolytic action (Wu et al. 2000).

The capacity of the novel neurite growth would be crucial to regenerate the nerves. In fact, the neurite regeneration must increase across the ECM at the injured location and re-innervate the distant targets (Pittman and DiBenedetto 1995). In present research, presence of an exogenous tPA in the structure composition increases the level of S100, NGF and BDNF that is related to the decreased generation of the collagen scar at the injured location. Such a condition can create a helpful micro-environment to grow the neurite growth and regenerate the nerves (Fredriksson et al. 2004). It should be mentioned that activating a number of growth factors like the brain-derived neurotrophic and platelet-derived growth factors is possible for tPA in order to augment the neurite outgrowth. Importantly, the existence of tPA has been followed by greater levels of NF expression, which possibly suggested a neurotrophic-like impact. However, if it has direct effects or influences by activating other factors should be additionally investigated elsewhere.

Therefore, according to the outputs, an exogenous tPA promote nerve regeneration after injury. In addition, the recombinant tPA has been the only medicine validated by the U.S. Food and Drug Administration for treating the thrombotic stroke. Finally, the positive impact on regenerating the peripheral nerves following damages occurred indicates an alternative promising tool for tPA.

Our experimental results of histology regenerated nerve fibers and substantially grew by the gap and linked distal and proximal nerve stumps in the tPA-loaded scaffold groups. Nevertheless, microscopic data and quantitative analysis of myelin thickness and axonal diameter showed that introducing tPA was able to regenerate nerve fibers.

Conclusion

In this study, the effect of tissue plasminogen activator on the sciatic nerve regeneration was investigated. This substance was loaded on the hydrophobic surface via plasma irradiation and characterized structurally and physically prior to in vivo evaluations. Afterwards, the structures were considered for the regeneration of 1-cm sciatic nerve defect of Rats in vivo assessments. Based on our finding presented herein, time-dependent decreases in SFI values were determined in the axotomy groups. The compound action potential amplitudes have been markedly decreased in gastrocnemius muscles of axotomy group. On the other hand, a remarkable reduction in the total volume of the spinal anterior horn was found in the axotomy group. In conclusion, applying tPA can result in regenerating the damaged peripheral nerve.

Acknowledgments Animal studies of this work were performed at Hearing Disorders Research Center, Loghman Hakim Medical Center, Shahid Beheshti University of Medical Sciences, Tehran, Iran. Therefore, In vivo part of this study is derived from the thesis formulated by Ensieh Sajadi, the MSc student at Department of Biology and Anatomical Sciences, School of Medicine, Shahid Beheshti University of Medical Sciences, Tehran, Iran (Registration No. 1397-270).

Author Contributions MAA and ES designed this study and provided the clinical data and sample. ARR and AR carried out the animal model and immunohistochemistry. AA performed the statistical analysis. RMF wrote and drafted the manuscript. MB and YS carried out the real-time PCR. All authors read and approved the final manuscript.

Funding Information This article was financially supported by the Hearing Disorders Research Center, Loghman Hakim Medical Center, Shahid Beheshti University of Medical Sciences, Tehran, Iran (grant number: 91-6124).

Compliance with Ethical Standards

Conflict of Interest The authors declare that they have no conflict of interest.

Ethical Approval All procedures were approved by the Medical Ethics Committee at Shahid Beheshti University of Medical Sciences, Tehran, Iran (IR.SBMU.MSP.REC. 1396.544).

References

- Akassoglou K, Kombrinck KW, Degen JL, Strickland S (2000) Tissue plasminogen activator-mediated fibrinolysis protects against axonal degeneration and demyelination after sciatic nerve injury. *J Cell Biol* 149(5):1157–1166
- Alvarez-Perez MA, Guarino V, Cirillo V, Ambrosio L (2010) Influence of gelatin cues in PCL electrospun membranes on nerve outgrowth. *Biomacromolecules* 11(9):2238–2246
- Böttcher H, Eisbrenner K, Fritz S, Kindermann G, Kraxner F, McCallum I, Obersteiner M (2009) An assessment of monitoring requirements and costs of ‘Reduced Emissions from Deforestation and Degradation’. *Carbon Balance and Management* 4(1):7

- Cao H, Liu T, Chew SY (2009) The application of nanofibrous scaffolds in neural tissue engineering. *Adv Drug Deliv Rev* 61(12):1055–1064
- Chew SY, Mi R, Hoke A, Leong KW (2008) The effect of the alignment of electrospun fibrous scaffolds on Schwann cell maturation. *Biomaterials* 29(6):653–661
- Chong EJ, Phan TT, Lim IJ, Zhang Y, Bay BH, Ramakrishna S, Lim CT (2007) Evaluation of electrospun PCL/gelatin nanofibrous scaffold for wound healing and layered dermal reconstitution. *Acta Biomater* 3(3):321–330
- Frattini F, Pereira Lopes FR, Almeida FM, Rodrigues RF, Boldrini LC, Tomaz MA, Baptista AF, Melo PA, Martinez AMB (2012) Mesenchymal stem cells in a polycaprolactone conduit promote sciatic nerve regeneration and sensory neuron survival after nerve injury. *Tissue Eng A* 18(19–20):2030–2039
- Fredriksson L, Li H, Fieber C, Li X, Eriksson U (2004) Tissue plasminogen activator is a potent activator of PDGF-CC. *EMBO J* 23(19):3793–3802
- García-Rocha M, Avila J, Armas-Portela R (1994) Tissue-type plasminogen activator (tPA) is the main plasminogen activator associated with isolated rat nerve growth cones. *Neurosci Lett* 180(2):123–126
- Ghasemi-Mobarakeh L, Prabhakaran MP, Morshed M, Nasr-Esfahani M-H, Ramakrishna S (2008) Electrospun poly (ϵ -caprolactone)/gelatin nanofibrous scaffolds for nerve tissue engineering. *Biomaterials* 29(34):4532–4539
- Grinsell, D. and C. Keating (2014). Peripheral nerve reconstruction after injury: a review of clinical and experimental therapies. *BioMed research international* 2014
- Gundersen H, Bagger P, Bendtsen T, Evans S, Korbo L, Marcussen N, Møller A, Nielsen K, Nyengaard J, Pakkenberg B (1988a) The new stereological tools: disector, fractionator, nucleator and point sampled intercepts and their use in pathological research and diagnosis. *Apmis* 96(7–12):857–881
- Gundersen H, Bendtsen TF, Korbo L, Marcussen N, Møller A, Nielsen K, Nyengaard J, Pakkenberg B, Sørensen FB, Vesterby A (1988b) Some new, simple and efficient stereological methods and their use in pathological research and diagnosis. *Apmis* 96(1–6):379–394
- Himes B, Tessler A (1989) Death of some dorsal root ganglion neurons and plasticity of others following sciatic nerve section in adult and neonatal rats. *J Comp Neurol* 284(2):215–230
- Hyun JK, Kim H-W (2010) Clinical and experimental advances in regeneration of spinal cord injury. *Journal of tissue engineering* 1(1):650857
- Jensen EB, Gundersen HJG, Østerby R (1979) Determination of membrane thickness distribution from orthogonal intercepts. *J Microsc* 115(1):19–33
- Johnson EO, Charchanti A, Soucacos PN (2008) Nerve repair: experimental and clinical evaluation of neurotrophic factors in peripheral nerve regeneration. *Injury* 39(3):37–42
- Karlsson LM, Cruz-Orive L (1997) Estimation of mean particle size from single sections. *J Microsc* 186(2):121–132
- Kim CH, Khil MS, Kim HY, Lee HU, Jahng KY (2006) An improved hydrophilicity via electrospinning for enhanced cell attachment and proliferation. *Journal of Biomedical Materials Research Part B: Applied Biomaterials: An Official Journal of The Society for Biomaterials, The Japanese Society for Biomaterials, and The Australian Society for Biomaterials and the Korean Society for Biomaterials* 78(2):283–290
- Koh H, Yong T, Chan C, Ramakrishna S (2008) Enhancement of neurite outgrowth using nano-structured scaffolds coupled with laminin. *Biomaterials* 29(26):3574–3582
- Larsen JO (1998) Stereology of nerve cross sections. *J Neurosci Methods* 85(1):107–118
- Lee CH, Shin HJ, Cho IH, Kang Y-M, Kim IA, Park K-D, Shin J-W (2005) Nanofiber alignment and direction of mechanical strain affect the ECM production of human ACL fibroblast. *Biomaterials* 26(11):1261–1270
- Li W-J, Cooper JA Jr, Mauck RL, Tuan RS (2006) Fabrication and characterization of six electrospun poly (α -hydroxy ester)-based fibrous scaffolds for tissue engineering applications. *Acta Biomater* 2(4):377–385
- Mataga N, Nagai N, Hensch TK (2002) Permissive proteolytic activity for visual cortical plasticity. *Proc Natl Acad Sci* 99(11):7717–7721
- Mayer M (1990) Biochemical and biological aspects of the plasminogen activation system. *Clin Biochem* 23(3):197–211
- Noorafshan A, Omidi A, Karbalay-Doust S (2011) Curcumin protects the dorsal root ganglion and sciatic nerve after crush in rat. *Pathology-Research and Practice* 207(9):577–582
- Noorafshan A, Hoseini L, Karbalay-Doust S, Nadimi E (2012) A simple stereological method for estimating the number and the volume of the pancreatic beta cells. *JOP Journal of the Pancreas* 13(4):427–432
- Pierucci A, de Oliveira ALR (2006) Increased sensory neuron apoptotic death 2 weeks after peripheral axotomy in C57BL/6J mice compared to A/J mice. *Neurosci Lett* 396(2):127–131
- Pittman RN, DiBenedetto AJ (1995) PC12 cells overexpressing tissue plasminogen activator regenerate neurites to a greater extent and migrate faster than control cells in complex extracellular matrix. *J Neurochem* 64(2):566–575
- Prabhakaran MP, Venugopal J, Chan CK, Ramakrishna S (2008) Surface modified electrospun nanofibrous scaffolds for nerve tissue engineering. *Nanotechnology* 19(45):455102
- Qian Z, Gilbert ME, Colicos MA, Kandel ER, Kuhl D (1993) Tissue-plasminogen activator is induced as an immediate-early gene during seizure, kindling and long-term potentiation. *Nature* 361(6411):453–457
- Rogove AD, Siao C, Keyt B, Strickland S, Tsirka SE (1999) Activation of microglia reveals a non-proteolytic cytokine function for tissue plasminogen activator in the central nervous system. *J Cell Sci* 112(22):4007–4016
- Schnell E, Klinkhammer K, Balzer S, Brook G, Klee D, Dalton P, Mey J (2007) Guidance of glial cell migration and axonal growth on electrospun nanofibers of poly- ϵ -caprolactone and a collagen/poly- ϵ -caprolactone blend. *Biomaterials* 28(19):3012–3025
- Seeds NW, Williams BL, Bickford PC (1995) Tissue plasminogen activator induction in Purkinje neurons after cerebellar motor learning. *Science* 270(5244):1992–1994
- Siconolfi LB, Seeds NW (2001) Mice lacking tPA, uPA, or plasminogen genes showed delayed functional recovery after sciatic nerve crush. *J Neurosci* 21(12):4348–4355
- Siemionow M, Brzezicki G (2009) Current techniques and concepts in peripheral nerve repair. *Int Rev Neurobiol* 87:141–172
- Soleimani M, Mahboudi F, Davoudi N, Amanzadeh A, Azizi M, Adeli A, Rastegar H, Barkhordari F, Mohajer-Maghari B (2007) Expression of human tissue plasminogen activator in the trypanosomatid protozoan *Leishmania tarentolae*. *Biotechnol Appl Biochem* 48(1):55–61
- Terenghi G (1999) Peripheral nerve regeneration and neurotrophic factors. *The Journal of Anatomy* 194(1):1–14
- Tsirka SE, Gualandris A, Amaral DG, Strickland S (1995) Excitotoxin-induced neuronal degeneration and seizure are mediated by tissue plasminogen activator. *Nature* 377(6547):340–344
- Tsirka SE, Rogove AD, Bugge TH, Degen JL, Strickland S (1997) An extracellular proteolytic cascade promotes neuronal degeneration in the mouse hippocampus. *J Neurosci* 17(2):543–552
- Varejão AS, Melo-Pinto P, Meek MF, Filipe VM, Bulas-Cruz J (2004) Methods for the experimental functional assessment of rat sciatic nerve regeneration. *Neurol Res* 26(2):186–194
- Vassalli J-D, Sappino A, Belin D (1991) The plasminogen activator/plasmin system. *J Clin Invest* 88(4):1067–1072
- Vestergaard S, Tandrup T, Jakobsen J (1997) Effect of permanent axotomy on number and volume of dorsal root ganglion cell bodies. *J Comp Neurol* 388(2):307–312

- Willerth SM, Sakiyama-Elbert SE (2007) Approaches to neural tissue engineering using scaffolds for drug delivery. *Adv Drug Deliv Rev* 59(4–5):325–338
- Wu YP, Siao C-J, Lu W, Sung T-C, Frohman MA, Milev P, Bugge TH, Degen JL, Levine JM, Margolis RU (2000) The tissue plasminogen activator (tPA/plasmin) extracellular proteolytic system regulates seizure-induced hippocampal mossy fiber outgrowth through a proteoglycan substrate. *J Cell Biol* 148(6):1295–1304
- Yang L, Fitie CF, van der Werf KO, Bennink ML, Dijkstra PJ, Feijen J (2008) Mechanical properties of single electrospun collagen type I fibers. *Biomaterials* 29(8):955–962
- Yepes M, Sandkvist M, Coleman TA, Moore E, Wu J-Y, Mitola D, Bugge TH, Lawrence DA (2002) Regulation of seizure spreading by neuroserpin and tissue-type plasminogen activator is plasminogen-independent. *J Clin Invest* 109(12):1571–1578
- Yu W, Zhao W, Zhu C, Zhang X, Ye D, Zhang W, Zhou Y, Jiang X, Zhang Z (2011) Sciatic nerve regeneration in rats by a promising electrospun collagen/poly (ϵ -caprolactone) nerve conduit with tailored degradation rate. *BMC Neurosci* 12(1):68
- Zalewski AA, Gulati AK (1981) Rejection of nerve allografts after cessation of immunosuppression with cyclosporin A. *Transplantation* 31(1):88–89

Publisher's Note Springer Nature remains neutral with regard to jurisdictional claims in published maps and institutional affiliations.